 CMES, vol.88, no.5, pp.325-350, 2012

Quasi-Conforming Triangular Reissner-Mindlin Shell Elements by Using Timoshenko's Beam Function

Changsheng Wang[1] **and Ping Hu**[1,2]

Abstract: Based on the Reissner-Mindlin plate theory, two 3-node triangular flat shell elements QCS31 and QCS32 are proposed by using Timoshenko's beam function within the framework of quasi-conforming technique. The exact displacement function of the Timoshenko's beam is used as the displacement on the element boundary in the bending part and the interpolated inner field function is also derived by the function. In the shear part the re-constitution technique is adopted. The drilling degrees of freedom are added in the membrane part to improve membrane behavior. The proposed elements can be used for the analysis of both moderately thick and thin plates/shells, and the convergence for the very thin case can be ensured theoretically. The integration of the elements is performed analytically and features an explicit form of the stiffness matrix, which is more precise and efficient from a mathematical point of view. The numerical tests and comparisons with other existing solutions in the literatures suggest that the present elements are competitive.

Keywords: quasi-conforming, Timoshenko's beam, flat shell.

1 Introduction

The wide application of shell structures in engineering has been aspiring numerous researchers to develop simple and efficient shell elements. Among different kinds of shell elements such as a flat shell element, a curved shell element and a degenerated solid element, the flat shell element is the most popular model for finite element analysis of shell structures as it is simple, easy to implement and computationally efficient. Generally, triangular flat shell elements consist of triangular membrane elements and triangular bending plate elements and possess capabilities

[1] School of Automotive Engineering, Faculty of Vehicle Engineering and Mechanics, State Key Laboratory of Structural Analysis for Industrial Equipment, Dalian University of Technology, Dalian 116024, P.R. China.
[2] pinghu@dlut.edu.cn

of bending and stretching deformation. Triangular elements are flexible as the convenience in modeling arbitrary shaped shell structures and the convergence to the exact geometry is obtained when the mesh is refined.

A large number of triangular flat shell elements have been developed over several decades. Among these, the membrane behavior of some elements is represented by CST or LST plane element. However, a drawback of both CST and LST elements is the lack of an in-plane rotational degree of freedom. As a result the stiffness matrix becomes singular when all elements intersecting at a node are coplanar and the local coordinate system coincides with the global coordinate system. To overcome this problem, Zienkiewicz [Zienkiewicz (1977)] and later Bathe and Ho [Bathe and Ho (1981)] proposed to use a fictitious stiffness. Allman [Allman (1991, 1994)] presented a triangular flat facet finite element for the analysis of general thin shells with six DOF's per vertex node that includes the drilling DOF. Allman's earlier development of a membrane element [Allman (1984)] with a drilling DOF was followed by a rich collection of contributions for both triangular and quadrilateral elements, such as Bergan and Fellipa [Bergan and Felippa (1985)], and its newest versions [Alvin, Fuente, Haugen, and Felippa (1992); Felippa and Militello (1992); Felippa and Alexander (1992)], Cook [Cook (1986, 1987)] and Allman [Allman (1988)]. A good review regarding this issue can be found in the paper by Felippa [Felippa (2003)] which compares the derivation methods for constructing triangular elements with corner drilling degrees of freedom.

Triangular flat shell elements consist of triangular membrane elements and triangular plate bending elements. Bazeley et al. [Bazeley, Cheung, Irons, and Zienkiewicz (1966)] developed conforming and nonconforming plate bending elements by using shape functions based on the area coordinates, which are named as BCIZ. The DKT(Discrete Kirchhoff Triangular) proposed by Batoz et al. [Batoz, Bathe, and Ho (1980)] based on the discrete Kirchhoff constraint may possibly be the most influential triangular bending element so far. Numerous plates/shells elements based on the discrete Kirchhoff constraint were developed later, such as the LOOF-DKL by Meek and Tan [Meek and Tan (1985)], the DKTP by Dhatt et al. [Dhatt, Marcotte, and Matte (1986)] and the DKMT by Katili [Katili (1993)]. Batoz et al. [Batoz, Zheng, and Hammadi (2001)] reviewed the discrete Kirchhoff flat shell elements for the linear analysis of plates and shells. However, C^1 continuity is required to secure interelement compatibility in the derivation of the elements based on the discrete Kirchhoff constraint. The plate elements based on Reissner-Mindlin plate theory are welcome because only C^0 continuity is required, and both thin and moderately thick plate can be simulated in one element model [Batoz and Lardeur (1989); Batoz and Katili (1992)]. The Reissner-Mindlin plate theory takes account of shear deformation by decoupling the rotation of plate cross-section from

the slope of the deformed mid-surface. However, when the thickness is decreasing, shear locking is observed. Commonly adopted techniques to handle shear locking are reduced/selective integration techniques [Zienkiewicz, Taylor, and Too (1971); Hughes, Cohen, and Haroun (1978)]. However, they may exhibit extra zero energy modes, and also produce oscillatory results for some problems. Several other approaches have been developed by researchers to overcome shear locking, such as the hybrid/mixed formulation [Lee and Plan (1978); Spilker and Munir (1980)], the assumed natural strain method (ANS) [MacNeal (1982); Bathe and Dvorkin (1986)], the enhanced assumed strain method (EAS) [Simo and Rifai (1990)] and nonconforming element method [Kim and Choi (1992); Brezzi and Marini (2003)].

Recently Chen and Cheung [Cheung and Chen (1995); Chen and Cheung (1997)] proposed a refined non-conforming element method (RNEM) to improve the performance of the non-conforming elements. In their work, the interelement displacement continuity was enforced in an average sense, which resulted in not only better convergence of the solution but also improvement of its accuracy. Based on the Reissner-Mindlin plate theory, they derived a series of quadrilateral plates/shells elements [Chen and Cheung (2000, 2005)] and triangular plates/shells elements [Chen and Cheung (2001); Ge and Chen (2003); Chen (2004)] by introducing the displacement function of the Timoshenko's beam function into the formulation. In [Ge and Chen (2003)], flat shell elements were formed by the assemblage of discrete Mindlin plate elements RDKTM [Chen and Cheung (2001)] and either the constant strain membrane element CST or the Allman's membrane element with drilling degrees [Allman (1984)]. Zhang et al. [Zhang, Zhou, Li, Feng, and Li (2011)] constructed a 3-node flat triangular shell element by combining the ANDED-based membrane component [Felippa (2003)] includes rotational degrees of freedom and the Mindlin plate element RDKTM [Chen and Cheung (2001)].

The Quasi-Conforming (QC) technique was proposed by Tang et al. [Tang, Chen, and Liu (1980)] to meet the challenge of inter-elements conforming problems. The strain-displacement equation is weakened as well as the equilibrium equation in QC method. The QC technique is a general finite element method in which multiple sets of approximating functions are used instead of the conventional single set of functions. The key to the QC elements is the choice of string net functions on the element boundary and the inner-field function [Tang, Chen, and Liu (1983)]. With appropriate initial assumed strain/displacement and string net functions, elements may be free from shear locking and membrane locking, spurious kinematic modes and numerical ill condition. For a summary of the development of the QC technique, the readers are referred to [Lomboy, Suthasupradit, Kim, and Oñate (2009)]. A number of efficient quadrilateral plates/shells elements are proposed within the framework of assumed strain QC technique, such as [Shi and Voyiadjis (1991);

Kim, Lomboy, and Voyiadjis (2003)]. Hu et al. [Hu, Xia, and Tang (2011)] developed the assumed displacement QC technique as a basic technique and constructed a 4-node Reissner-Mindlin shell element by using the interpolation functions proposed by Shi and Voyiadjis [Shi and Voyiadjis (1991)]. The assumed displacements QC technique can give a simple and rational choice of initial strains which will be derived from the truncated Taylor expansion of displacements and the complicated process of rank analysis [Liu, Shi, and Tang (1983)] in assumed strain QC technique can be avoided. Wang et al. [Wang, Hu, and Xia (2012)] constructed a new quadrilateral QC flat shell element by deducing a series of new interpolation functions. The differences between the assumed strain QC technique and the assumed displacement QC technique are detailed in [Hu, Xia, and Tang (2011); Wang, Hu, and Xia (2012)].

Few QC triangular plates/shells elements based on the Reissner-Mindlin plate theory are developed. Most proposed QC triangular plates/shells elements are based on the Kirchhoff assumption, such as [Tang, Chen, and Liu (1981); Lv and Xu (1989)]. Some of the quadrilateral QC elements could degenerate to the triangular elements, however, the accuracy reduce rapidly for that the interpolation functions for the quadrilateral element is not appropriate for the triangular element. A 4-node quadrilateral flat shell element by using Timoshenko's beam function is developed in [Wang, Hu, and Xia (2012)]. In this paper, we use Timoshenko's beam function to deduce triangular flat shell elements. The contribution of the paper is that a series of new interpolation functions are deduced for the triangular QC technique, including the string net functions and inner-field functions. Moreover, the inner-field function of the bending part is interpolated to the nodes. The re-constitution technique for the shear strain terms is adopted for shear part. Both shell elements have an explicit stiffness matrix, which is computationally efficient. Numerical examples are present to validate the shell elements. The test results show very good performance when compared with references.

2 Element stiffness matrix

For deriving the element stiffness matrix of Reissner-Mindlin shell element, the strain energy in an element can be written in the following decomposed bending, shear and membrane modes as

$$\pi = \iint_{\Omega} (\frac{1}{2}\boldsymbol{\varepsilon}_b^T \mathbf{D}_b \boldsymbol{\varepsilon}_b + \frac{1}{2}\boldsymbol{\varepsilon}_s^T \mathbf{D}_s \boldsymbol{\varepsilon}_s + \frac{1}{2}\boldsymbol{\varepsilon}_m^T \mathbf{D}_m \boldsymbol{\varepsilon}_m) dxdy \tag{1}$$

in which $\boldsymbol{\varepsilon}_b$, $\boldsymbol{\varepsilon}_s$ and $\boldsymbol{\varepsilon}_m$ are the bending strain vector, transverse shear strain vector and membrane strain vector respectively

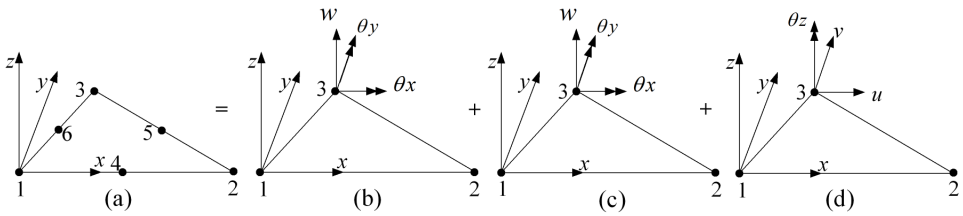

Figure 1: The element composition: (a) the flat shell element with surplus mid-nodes; (b) the bending part; (c) the shear part; (d) the membrane part.

$$\boldsymbol{\varepsilon}_b = \begin{pmatrix} \dfrac{\partial \theta_y}{\partial x} \\ -\dfrac{\partial \theta_x}{\partial y} \\ \dfrac{\partial \theta_y}{\partial y} - \dfrac{\partial \theta_x}{\partial x} \end{pmatrix} \quad \boldsymbol{\varepsilon}_s = \begin{pmatrix} \dfrac{\partial w}{\partial x} + \theta_y \\ \dfrac{\partial w}{\partial y} - \theta_x \end{pmatrix} \quad \boldsymbol{\varepsilon}_m = \begin{pmatrix} \dfrac{\partial u}{\partial x} \\ \dfrac{\partial v}{\partial y} \\ \dfrac{\partial u}{\partial y} + \dfrac{\partial v}{\partial x} \end{pmatrix} \tag{2}$$

$\mathbf{D}_b$,$\mathbf{D}_s$ and $\mathbf{D}_m$ are the elasticity matrices

$$\mathbf{D}_b = \frac{Et^3}{12(1-v^2)} \begin{pmatrix} 1 & v & 0 \\ v & 1 & 0 \\ 0 & 0 & \frac{1-v}{2} \end{pmatrix}$$

$$\mathbf{D}_s = \frac{5Et}{12(1+v)} \begin{pmatrix} 1 & 0 \\ 0 & 1 \end{pmatrix} \quad \mathbf{D}_m = \frac{Et}{1-v^2} \begin{pmatrix} 1 & v & 0 \\ v & 1 & 0 \\ 0 & 0 & \frac{1-v}{2} \end{pmatrix} \tag{3}$$

The bending part, the shear part and the membrane part can be combined to form a 3-node flat shell element, as shown in Figure 1.

In the QC technique, the element strain fields are approximated using polynomials and integrated using string net functions. To keep the shell element stiffness matrix rank sufficient and free from spurious kinematic modes, the strain vectors can be approximated as in the [Wang, Hu, and Xia (2012)] as follows:

$$\boldsymbol{\varepsilon}_b = \begin{pmatrix} 0 & 0 & 0 & 0 & 0 & 1 & 0 & 2x & y & 0 \\ 0 & 1 & 0 & x & 2y & 0 & 0 & 0 & 0 & 0 \\ 1 & 0 & 2x & y & 0 & 0 & 1 & 0 & x & 2y \end{pmatrix} \begin{pmatrix} a_1 \\ \vdots \\ a_5 \\ b_1 \\ \vdots \\ b_5 \end{pmatrix} = \mathbf{Q}_b \boldsymbol{\alpha}_b \tag{4}$$

$$\boldsymbol{\varepsilon}_s = \begin{pmatrix} 1 & 0 \\ 0 & 1 \end{pmatrix} \begin{pmatrix} c_1 \\ c_2 \end{pmatrix} = \mathbf{Q}_s \boldsymbol{\alpha}_s \tag{5}$$

$$\boldsymbol{\varepsilon}_m = \begin{pmatrix} 1 & 0 & 2x & y & 0 & 0 & 0 & 0 & 0 & 0 \\ 0 & 0 & 0 & 0 & 0 & 0 & 1 & 0 & x & 2y \\ 0 & 1 & 0 & x & 2y & 1 & 0 & 2x & y & 0 \end{pmatrix} \begin{pmatrix} d_1 \\ \vdots \\ d_5 \\ e_1 \\ \vdots \\ d_5 \end{pmatrix} = \mathbf{Q}_m \boldsymbol{\alpha}_m \tag{6}$$

in which $\boldsymbol{\alpha}_b$, $\boldsymbol{\alpha}_s$ and $\boldsymbol{\alpha}_m$ are the undetermined element strain parameter vectors. Letting $\mathbf{Q}_b^T$, $\mathbf{Q}_s^T$ and $\mathbf{Q}_m^T$ be the test function ,then

$$\iint_\Omega \mathbf{Q}_b^T \mathbf{Q}_b dxdy \boldsymbol{\alpha}_b = \iint_\Omega \mathbf{Q}_b^T \boldsymbol{\varepsilon}_b dxdy \tag{7}$$

$$\iint_\Omega \mathbf{Q}_s^T \mathbf{Q}_s dxdy \boldsymbol{\alpha}_s = \iint_\Omega \mathbf{Q}_s^T \boldsymbol{\varepsilon}_s dxdy \tag{8}$$

$$\iint_\Omega \mathbf{Q}_m^T \mathbf{Q}_m dxdy \boldsymbol{\alpha}_m = \iint_\Omega \mathbf{Q}_m^T \boldsymbol{\varepsilon}_m dxdy \tag{9}$$

where Ω represents the element domain. The element strain parameter vectors $\boldsymbol{\alpha}_b$, $\boldsymbol{\alpha}_s$ and $\boldsymbol{\alpha}_m$ can be determined in terms of the element nodal displacement vector $\mathbf{q}$

$$\boldsymbol{\alpha}_b = \mathbf{A}_b^{-1} \mathbf{C}_b \mathbf{q} \quad \boldsymbol{\alpha}_s = \mathbf{A}_s^{-1} \mathbf{C}_s \mathbf{q} \quad \boldsymbol{\alpha}_m = \mathbf{A}_m^{-1} \mathbf{C}_m \mathbf{q} \tag{10}$$

in which

$$\mathbf{A}_b = \iint_\Omega \mathbf{Q}_b^T \mathbf{Q}_b dxdy \quad \mathbf{A}_s = \iint_\Omega \mathbf{Q}_s^T \mathbf{Q}_s dxdy \quad \mathbf{A}_m = \iint_\Omega \mathbf{Q}_m^T \mathbf{Q}_m dxdy \tag{11}$$

$$\mathbf{C}_b \mathbf{q} = \iint_\Omega \mathbf{Q}_b^T \boldsymbol{\varepsilon}_b dxdy \quad \mathbf{C}_s \mathbf{q} = \iint_\Omega \mathbf{Q}_s^T \boldsymbol{\varepsilon}_s dxdy \quad \mathbf{C}_m \mathbf{q} = \iint_\Omega \mathbf{Q}_m^T \boldsymbol{\varepsilon}_m dxdy \tag{12}$$

$$\mathbf{q} = \begin{pmatrix} u_1 & v_1 & w_1 & \theta_{x1} & \theta_{y1} & \theta_{z1} & \dots & u_3 & v_3 & w_3 & \theta_{x3} & \theta_{y3} & \theta_{z3} \end{pmatrix}^T \tag{13}$$

Substituting equation (10) into equations (4)(5)(6) respectively, we obtain the element strain vectors expressed in terms of the element nodal displacement vector $\mathbf{q}$

$$\begin{aligned} \boldsymbol{\varepsilon}_b &= \mathbf{Q}_b \boldsymbol{\alpha}_b = \mathbf{Q}_b \mathbf{A}_b^{-1} \mathbf{C}_b \mathbf{q} = \mathbf{B}_b \mathbf{q} \\ \boldsymbol{\varepsilon}_s &= \mathbf{Q}_s \boldsymbol{\alpha}_s = \mathbf{Q}_s \mathbf{A}_s^{-1} \mathbf{C}_s \mathbf{q} = \mathbf{B}_s \mathbf{q} \\ \boldsymbol{\varepsilon}_m &= \mathbf{Q}_m \boldsymbol{\alpha}_m = \mathbf{Q}_m \mathbf{A}_m^{-1} \mathbf{C}_m \mathbf{q} = \mathbf{B}_m \mathbf{q} \end{aligned} \tag{14}$$

Consequently, the element stiffness matrix can be obtain by substituting equation (14) into equation (1)

$$\mathbf{K} = \mathbf{K}_b + \mathbf{K}_s + \mathbf{K}_m \tag{15}$$

where $\mathbf{K}_b$, $\mathbf{K}_s$ and $\mathbf{K}_m$ are the element bending, shear and membrane stiffness matrices respectively, and they are defined as

$$\begin{aligned}
\mathbf{K}_b &= \iint_\Omega \mathbf{B}_b^T \mathbf{D}_b \mathbf{B}_b dxdy = \mathbf{C}_b^T \mathbf{A}_b^{-T} \iint_\Omega \mathbf{Q}_b^T \mathbf{D}_b \mathbf{Q}_b dxdy \mathbf{A}_b^{-1} \mathbf{C}_b \\
\mathbf{K}_s &= \iint_\Omega \mathbf{B}_s^T \mathbf{D}_s \mathbf{B}_s dxdy = \mathbf{C}_s^T \mathbf{A}_s^{-T} \iint_\Omega \mathbf{Q}_s^T \mathbf{D}_s \mathbf{Q}_s dxdy \mathbf{A}_s^{-1} \mathbf{C}_s \\
\mathbf{K}_m &= \iint_\Omega \mathbf{B}_m^T \mathbf{D}_m \mathbf{B}_m dxdy = \mathbf{C}_m^T \mathbf{A}_m^{-T} \iint_\Omega \mathbf{Q}_m^T \mathbf{D}_m \mathbf{Q}_m dxdy \mathbf{A}_m^{-1} \mathbf{C}_m
\end{aligned} \tag{16}$$

The integrals of the polynomials in equations (11) and (16) can be carried out quite easily, and the essential work is the evaluation of the matrices $\mathbf{C}_b$, $\mathbf{C}_s$ and $\mathbf{C}_m$ defined in equation (12).

3 The evaluation of element strain fields

The Timoshenko's beam function can be used to derive efficient Reissner-Mindlin plates/shells elements, such as [Chen and Cheung (2000, 2005, 2001); Ge and Chen (2003); Chen (2004); Zhang, Zhou, Li, Feng, and Li (2011)]. which can be expressed as follows,

$$\begin{aligned}
w = &(L_1 + \mu_e L_1 L_2 (L_1 - L_2)) w_1 + (L_1 L_2 + \mu_e L_1 L_2 (L_1 - L_2)) L/2 \theta_1 \\
&+ (L_2 + \mu_e L_1 L_2 (L_2 - L_1)) w_2 + (-L_1 L_2 + \mu_e L_1 L_2 (L_1 - L_2)) L/2 \theta_2
\end{aligned} \tag{17}$$

$$\theta = -(6 L_1 L_2 / L) \mu_e w_1 + L_1 (1 - 3 \mu_e L_2) \theta_1 + (6 L_1 L_2 / L) \mu_e w_2 + L_2 (1 - 3 \mu_e L_1) \theta_2 \tag{18}$$

in which $L_1 = 1 - s/L$, $L_2 = s/L$, $\mu_e = 1/(1 + 12\lambda_e)$, $\lambda_e = t^2/5(1-v)L^2$. L is the length of the beam, t is the height of the beam, v is Poisson's ratio.

3.1 C_b for bending part

In order to calculate the matrix $\mathbf{C}_b$ in equation (12), the integrals involving $\partial \theta_x / \partial x$ are concerned as example. By using the Green's theorem we obtain

$$\begin{aligned}
\iint_\Omega \frac{\partial \theta_x}{\partial x} dxdy &= \oint_s \theta_x n_x ds \\
\iint_\Omega \frac{\partial \theta_x}{\partial x} x dxdy &= \oint_s \theta_x n_x x ds - \iint_\Omega \theta_x dxdy \\
\iint_\Omega \frac{\partial \theta_x}{\partial x} y dxdy &= \oint_s \theta_x n_x y ds
\end{aligned} \tag{19}$$

For the boundary integration, the following transformation equations are needed

$$\begin{pmatrix} \theta_x \\ \theta_y \end{pmatrix} = \begin{pmatrix} n_x & -n_y \\ n_y & n_x \end{pmatrix} \begin{pmatrix} \theta_s \\ \theta_n \end{pmatrix} \tag{20}$$

where $n_x = \cos(\mathbf{n}, \mathbf{x})$, $n_y = \cos(\mathbf{n}, \mathbf{y})$. Then the tangential rotation angles are chosen as the Timoshenko's beam function and the normal rotation angles are chosen as a linear function. For instance, along the 1-2 boundary

$$\theta_s = -(6L_1L_2/S_1)\mu_1 w_1 + L_1(1-3\mu_1 L_2)\theta_{s1} + (6L_1L_2/S_1)\mu_1 w_2 + L_2(1-3\mu_1 L_1)\theta_{s2} \tag{21}$$

$$\theta_n = L_1\theta_{n1} + L_2\theta_{n2} \tag{22}$$

$$\mu_1 = \frac{1}{1+12\lambda_1} \quad \lambda_1 = \frac{t^2}{5S_1^2(1-v)} \tag{23}$$

where $L_1 = 1 - s/S_1$, $L_2 = s/S_1$, s is the co-ordinate along the boundary, and S_1 is the 1-2 boundary length, θ_{si} and θ_{ni} are the tangential and normal slopes at the node $i(i = 1,2)$ on the boundary. It is obvious that the displacement θ_s shown in equation (21) on the boundary will become the displacement of a thin-plate boundary because $\lambda_1 \to 0$ when $t/S_1 \to 0$.

As the procedure of the RDKTM element, the explicit expression of inner-field displacement in the bending part can be obtain by eliminating the surplus parameters at the mid-side nodes as shown in Figure 1(a).

$$\begin{pmatrix} \theta_x \\ \theta_y \end{pmatrix} = \tilde{\mathbf{N}}\mathbf{q}_b \tag{24}$$

where

$$\mathbf{q}_b = \begin{pmatrix} w_1 & \theta_{x1} & \theta_{y1} & w_2 & \theta_{x2} & \theta_{y2} & w_3 & \theta_{x3} & \theta_{y3} \end{pmatrix}^T \tag{25}$$

$\tilde{\mathbf{N}}$ is defined as $\tilde{\mathbf{N}} = \begin{pmatrix} \tilde{\mathbf{N}}_1 & \tilde{\mathbf{N}}_2 & \tilde{\mathbf{N}}_3 \end{pmatrix}$ and

$$\tilde{\mathbf{N}}_j = \begin{pmatrix} P_j & P_{xj} & P_{yj} \\ R_j & R_{xj} & R_{yj} \end{pmatrix} \tag{26}$$

for shape function $\tilde{\mathbf{N}}_1$

$$
\begin{aligned}
P_1 &= -\frac{3}{2}\left(\frac{N_4 n_{x1}\mu_1}{S_1} - \frac{N_6 n_{x3}\mu_3}{S_3}\right) \\
P_{x1} &= N_1 + N_4\left(\frac{1}{2} - \frac{3}{4}n_{x1}^2\mu_1\right) + N_6\left(\frac{1}{4}n_{x1}n_{x3}(2-3\mu_3) + \frac{1}{2}n_{y1}n_{y3}\right) \\
P_{y1} &= N_4\left(-\frac{3}{4}n_{x1}n_{y1}\mu_1\right) + N_6\left(\frac{1}{4}n_{x3}n_{y1}(2-3\mu_3) - \frac{1}{2}n_{y3}n_{x1}\right) \\
R_1 &= -\frac{3}{2}\left(\frac{N_4 n_{y1}\mu_1}{S_1} - \frac{N_6 n_{y3}\mu_3}{S_3}\right) \\
R_{x1} &= N_4\left(-\frac{3}{4}n_{x1}n_{y1}\mu_1\right) + N_6\left(\frac{1}{4}n_{x1}n_{y3}(2-3\mu_3) - \frac{1}{2}n_{x3}n_{y1}\right) \\
R_{y1} &= N_1 + N_4\left(\frac{1}{2} - \frac{3}{4}n_{y1}^2\mu_1\right) + N_6\left(\frac{1}{4}n_{y1}n_{y3}(2-3\mu_3) + \frac{1}{2}n_{x1}n_{x3}\right)
\end{aligned}
\tag{27}
$$

where N_i is the shape function of the 6-node triangular element in area co-ordinates (ξ_i)

$$
\begin{aligned}
&N_i = (2\xi_i - 1)\xi_i \quad (i = 1,2,3) \\
&N_k = 4\xi_i\xi_j \quad (k = 4,5,6;\ ij = 12,23,31)
\end{aligned}
\tag{28}
$$

Other two shape functions $\tilde{\mathbf{N}}_i (i = 2,3)$ can be obtained by cyclic expressions. Then the inner-field integration in equation (19) can be calculated.

3.2 C_s for shear part

In order to calculate the matrix $\mathbf{C}_s$, the following integrations are considered:

$$
\iint_\Omega \left(\frac{\partial w}{\partial x} + \theta_y\right) dxdy \quad \iint_\Omega \left(\frac{\partial w}{\partial y} - \theta_x\right) dxdy \tag{29}
$$

The transverse shear strain of the element can be written as

$$
\boldsymbol{\varepsilon}_s = \begin{pmatrix} \gamma_x \\ \gamma_y \end{pmatrix} = \begin{pmatrix} \dfrac{\partial w}{\partial x} + \theta_y \\ \dfrac{\partial w}{\partial y} - \theta_x \end{pmatrix} \tag{30}
$$

$$
\begin{pmatrix} \gamma_x \\ \gamma_y \end{pmatrix} = \begin{pmatrix} \xi_1 & 0 & \xi_2 & 0 & \xi_3 & 0 \\ 0 & \xi_1 & 0 & \xi_2 & 0 & \xi_3 \end{pmatrix} \begin{pmatrix} \gamma_{x1} \\ \gamma_{y1} \\ \gamma_{x2} \\ \gamma_{y2} \\ \gamma_{x3} \\ \gamma_{y3} \end{pmatrix} \tag{31}
$$

In order to eliminate the shear locking, the Timoshenko's beam function is used to express the rotation and deflection on the boundaries. Such as the 1-2 boundary

$$\tilde{\theta}_s = -(6L_1L_2/S_1)\mu_1 w_1 + L_1(1-3\mu_1 L_2)\theta_{s1} + (6L_1L_2/S_1)\mu_1 w_2 + L_2(1-3\mu_1 L_1)\theta_{s2} \quad (32)$$

$$\begin{aligned}\tilde{w} = {} & (L_1+\mu_1 L_1 L_2(L_1-L_2))w_1 + (L_1L_2+\mu_1 L_1 L_2(L_1-L_2))S_1/2\theta_{s1} \\ & + (L_2+\mu_1 L_1 L_2(L_2-L_1))w_2 + (-L_1L_2+\mu_1 L_1 L_2(L_1-L_2))S_1/2\theta_{s2}\end{aligned} \quad (33)$$

Thus we obtain

$$\begin{aligned}\frac{\partial \tilde{w}}{\partial s} = {} & \frac{1}{S_1}(-1+\mu_1(1-6L_1L_2))w_1 + \frac{1}{2}(L_1-L_2+\mu_1(1-6L_1L_2))\theta_{s1} \\ & + \frac{1}{S_1}(1-\mu_1(1-6L_1L_2))w_2 + \frac{1}{2}(-L_1+L_2+\mu_1(1-6L_1L_2))\theta_{s2}\end{aligned} \quad (34)$$

The displacement $\tilde{\theta}_s - \partial\tilde{w}/\partial s$ shown in equations (32) and (34) will stay constant on the boundary due to

$$\tilde{\theta}_s - \frac{\partial \tilde{w}}{\partial s} = \frac{1}{S_1}(1-\mu_1)w_1 + \frac{1}{2}(1-\mu_1)\theta_{s1} - \frac{1}{S_1}(1-\mu_1)w_2 + \frac{1}{2}(1-\mu_1)\theta_{s2} \quad (35)$$

Thus the shear strains at node $i(i=1,2,3)$ can be expressed by the constant shear strains γ_{sj}. For node 1, there exists

$$\begin{pmatrix} \gamma_{s4} \\ \gamma_{s6} \end{pmatrix} = \begin{pmatrix} n_{x1} & n_{y1} \\ n_{x3} & n_{y3} \end{pmatrix} \begin{pmatrix} \gamma_{x1} \\ \gamma_{y1} \end{pmatrix} \quad (36)$$

and

$$\begin{pmatrix} \gamma_{x1} \\ \gamma_{y1} \end{pmatrix} = \frac{1}{n_{x1}n_{y3} - n_{y1}n_{x3}} \begin{pmatrix} n_{y3} & -n_{y1} \\ -n_{x3} & n_{x1} \end{pmatrix} \begin{pmatrix} \gamma_{s4} \\ \gamma_{s6} \end{pmatrix} \quad (37)$$

Similarly, other nodal shear strains γ_{xj} and γ_{yj} $(j=2,3)$ can be obtained by cyclic expressions. Finally, the transverse shear strain can be written as

$$\begin{pmatrix} \gamma_x \\ \gamma_y \end{pmatrix} = \tilde{\mathbf{N}}_s \begin{pmatrix} \gamma_{s4} \\ \gamma_{s5} \\ \gamma_{s6} \end{pmatrix} \quad (38)$$

in which

$$\tilde{\mathbf{N}}_s = \begin{pmatrix} n_{y3}\xi_1/A_1 - n_{y2}\xi_2/A_2 & n_{y1}\xi_2/A_2 - n_{y3}\xi_3/A_3 & n_{y2}\xi_3/A_3 - n_{y1}\xi_1/A_1 \\ n_{x2}\xi_2/A_2 - n_{x3}\xi_1/A_1 & n_{x3}\xi_3/A_3 - n_{x1}\xi_2/A_2 & n_{x1}\xi_1/A_1 - n_{x2}\xi_3/A_3 \end{pmatrix}$$

(39)

$$\begin{aligned} A_1 &= n_{x1}n_{y3} - n_{y1}n_{x3} \\ A_2 &= n_{x2}n_{y1} - n_{y2}n_{x1} \\ A_3 &= n_{x3}n_{y2} - n_{y3}n_{x2} \end{aligned} \tag{40}$$

and γ_{si} $(i = 4,5,6)$ are the natural shear strains at mid-side nodes $4,5,6$ of the element. This means that the shear strains can be expressed as follows

$$\begin{pmatrix} \gamma_{s4} \\ \gamma_{s5} \\ \gamma_{s6} \end{pmatrix} = \begin{pmatrix} \theta_{s4} - w_{,s4} \\ \theta_{s5} - w_{,s5} \\ \theta_{s6} - w_{,s6} \end{pmatrix} \tag{41}$$

Substituting $L_1 = L_2 = 0.5$ into equations (32) and (34), the θ_{s4} and $w_{,s4}$ at the mid-node 4 on the 1-2 boundary can be obtained as follows

$$\theta_{s4} = -\frac{3}{2S_1}\mu_1 w_1 + \frac{1}{4}(2-3\mu_1)\theta_{s1} + \frac{3}{2S_1}\mu_1 w_2 + \frac{1}{4}(2-3\mu_1)\theta_{s2} \tag{42}$$

$$w_{,s4} = -\frac{1}{2S_1}(2+\mu_1)w_1 - \frac{1}{4}\mu_1\theta_{s1} + \frac{1}{2S_1}(2+\mu_1)w_2 - \frac{1}{4}\mu_1\theta_{s2} \tag{43}$$

where θ_{sj} at the node $j(j = 1,2)$ on the 1-2 boundary can be expressed as

$$\theta_{sj} = \begin{pmatrix} n_{x1} & n_{y1} \end{pmatrix} \begin{pmatrix} \theta_{xj} \\ \theta_{yj} \end{pmatrix} \quad (j = 1,2) \tag{44}$$

Then $\theta_{s4} - w_{,s4}$ can be expressed by

$$\theta_{s4} - w_{,s4} = \mathbf{B}_{s1}\mathbf{q}_s \tag{45}$$

$$\mathbf{B}_{s1} = \begin{pmatrix} \dfrac{1-\mu_1}{S_1} & \dfrac{1}{2}n_{x1}(1-\mu_1) & \dfrac{1}{2}n_{y1}(1-\mu_1) & & & \\ -\dfrac{1-\mu_1}{S_1} & \dfrac{1}{2}n_{x2}(1-\mu_1) & \dfrac{1}{2}n_{y2}(1-\mu_1) & 0 & 0 & 0 \end{pmatrix} \tag{46}$$

in which, $\mathbf{q}_s$ is defined as

$$\mathbf{q}_s = \begin{pmatrix} w_1 & \theta_{x1} & \theta_{y1} & w_2 & \theta_{x2} & \theta_{y2} & w_3 & \theta_{x3} & \theta_{y3} \end{pmatrix}^T \tag{47}$$

Similarly, other mid-node parameters $\theta_{si} - w_{,si}$ $(i = 5,6)$ can be obtained in terms of the nodal parameter vector $\mathbf{q}_s$

$$\theta_{s5} - w_{,s5} = \mathbf{B}_{s2}\mathbf{q}_s \qquad \theta_{s6} - w_{,s6} = \mathbf{B}_{s3}\mathbf{q}_s \tag{48}$$

$$\begin{aligned}
\mathbf{B}_{s2} &= \begin{pmatrix} 0 & 0 & 0 & \dfrac{1-\mu_2}{S_2} & \dfrac{1}{2}n_{x2}(1-\mu_2) & \dfrac{1}{2}n_{y2}(1-\mu_2) \\ \dfrac{\mu_2-1}{S_2} & \dfrac{1}{2}n_{x3}(1-\mu_2) & \dfrac{1}{2}n_{y3}(1-\mu_2) \end{pmatrix} \\
\mathbf{B}_{s3} &= \begin{pmatrix} \dfrac{\mu_3-1}{S_3} & \dfrac{1}{2}n_{x1}(1-\mu_3) & \dfrac{1}{2}n_{y1}(1-\mu_3) & 0 & 0 & 0 \\ \dfrac{1-\mu_3}{S_3} & \dfrac{1}{2}n_{x3}(1-\mu_3) & \dfrac{1}{2}n_{y3}(1-\mu_3) \end{pmatrix}
\end{aligned} \tag{49}$$

Therefore, the transverse shear strains of the element can be obtained as follows

$$\boldsymbol{\varepsilon}_s = \begin{pmatrix} \dfrac{\partial w}{\partial x} + \theta_y \\ \dfrac{\partial w}{\partial y} - \theta_x \end{pmatrix} = \tilde{\mathbf{N}}_s \begin{pmatrix} \theta_{s4} - w_{,s4} \\ \theta_{s5} - w_{,s5} \\ \theta_{s6} - w_{,s6} \end{pmatrix} = \tilde{\mathbf{N}}_s \mathbf{B}_s \mathbf{q}_s \tag{50}$$

where

$$\mathbf{B}_s = \begin{pmatrix} \mathbf{B}_{s1} & \mathbf{B}_{s2} & \mathbf{B}_{s3} \end{pmatrix}^T \tag{51}$$

Finally the integration in equation (29) can be calculated, and the matrix $\mathbf{C}_s$ can be obtained.

3.3 C_m for membrane part

Now we calculate the matrix $\mathbf{C}_m$ in equation (12), and the following integrations are concerned

$$\begin{aligned}
&\iint_\Omega \frac{\partial u}{\partial x} dxdy = \oint_s u n_x ds \\
&\iint_\Omega \frac{\partial u}{\partial x} x dxdy = \oint_s u n_x x ds - \iint_\Omega u dxdy \\
&\iint_\Omega \frac{\partial u}{\partial x} y dxdy = \oint_s u n_x y ds
\end{aligned} \tag{52}$$

Two sets of interpolation functions are used here to calculate the stiffness matrix of the membrane part, and the constructed shell elements are named as ***QCS31*** and ***QCS32***.

QCS31 Along the element boundary 1-2, the string net functions are chosen as

$$\begin{aligned}
u &= L_1 u_1 + L_2 u_2 \\
v &= L_1 v_1 + L_2 v_2
\end{aligned} \tag{53}$$

and the interpolation functions for inner-field displacements are chosen as

$$\begin{aligned} u =& \xi_1 u_1 + \xi_2 u_2 + \xi_3 u_3 \\ v =& \xi_1 v_1 + \xi_2 v_2 + \xi_3 v_3 \end{aligned} \tag{54}$$

The drilling stiffness is considered in order to improve the membrane behavior. The strain energy for an element with true drilling rotation can be written as

$$\pi_t = \beta \frac{Et}{2(1-\nu^2)} \iint_\Omega \boldsymbol{\varepsilon}_t^2 dxdy \tag{55}$$

where t is the thickness of the shell, β is chosen to be equal to 0.0001 by numerical trials, and $\boldsymbol{\varepsilon}_t$ is the drilling strain defined as

$$\boldsymbol{\varepsilon}_t = \theta_z - \frac{1}{2}(\frac{\partial v}{\partial x} - \frac{\partial u}{\partial y}) \tag{56}$$

We assume $\boldsymbol{\varepsilon}_t$ as a constant strain field, then $\mathbf{Q}_t = 1$, $\mathbf{A}_t = \iint_\Omega dxdy$, and

$$\mathbf{C}_t \mathbf{q} = \iint_\Omega \theta_z - \frac{1}{2}(\frac{\partial v}{\partial x} - \frac{\partial u}{\partial y}) dxdy = \iint_\Omega \theta_z dxdy - \frac{1}{2}\oint_s (vn_x - un_y) ds \tag{57}$$

The string net functions and the inner-field displacements are chosen as equations (53) and (54).

QCS32 Along the element boundary 1-2, the string net functions are chosen as the Allman type functions [Allman (1984)]

$$\begin{aligned} u =& L_1 u_1 + L_2 u_2 + \frac{1}{4}(y_2 - y_1)(\theta_{z2} - \theta_{z1}) L_1 L_2 \\ v =& L_1 v_1 + L_2 v_2 - \frac{1}{4}(x_2 - x_1)(\theta_{z2} - \theta_{z1}) L_1 L_2 \end{aligned} \tag{58}$$

The interpolation functions for inner-field displacement are chosen as

$$\begin{aligned} u =& \xi_1 u_1 + \xi_2 u_2 + \xi_3 u_3 + \frac{1}{2}(y_2 - y_1)(\theta_{z2} - \theta_{z1})\xi_1 \xi_2 \\ &+ \frac{1}{2}(y_3 - y_2)(\theta_{z3} - \theta_{z2})\xi_2 \xi_3 + \frac{1}{2}(y_1 - y_3)(\theta_{z1} - \theta_{z3})\xi_3 \xi_1 \\ v =& \xi_1 v_1 + \xi_2 v_2 + \xi_3 v_3 + \frac{1}{2}(x_1 - x_2)(\theta_{z2} - \theta_{z1})\xi_1 \xi_2 \\ &+ \frac{1}{2}(x_2 - x_3)(\theta_{z3} - \theta_{z2})\xi_2 \xi_3 + \frac{1}{2}(x_3 - x_1)(\theta_{z1} - \theta_{z3})\xi_3 \xi_1 \end{aligned} \tag{59}$$

4 Numerical examples

In the section, several benchmark problems are presented to validate and demonstrate the performance of the flat shell elements. The results are compared with other plates/shells elements. The list of plate elements used for comparison is outlined in Table 1 and some flat shell elements are used for comparison list below.

DKT18(P): The triangular flat shell element formed by the plate element DKT and triangular membrane elements proposed by Allman [Allman (1984)];

DKT18(T): The triangular flat shell element formed by the plate element DKT and the constant strain membrane element CST with true drilling rotations;

RDKTM18(P): Refined triangular flat shell element formed by the plate element RDKTM and triangular membrane elements [Ge and Chen (2003)];

RDKTM18(T): Refined triangular flat shell element formed by the plate element RDKTM and the constant strain membrane element CST with true drilling rotations [Ge and Chen (2003)].

Table 1: List of plate elements used for comparison

Name	Description
T3-R	The reduced/selective integration triangular element[Pugh and Zienkiewicz (1978)]
T3	The triangular displacement element with full integration
DST-BL	Discrete Mindlin triangular plate element proposed by Batoz and Lardeur [Batoz and Lardeur (1989)]
DST-BK	Discrete Mindlin triangular plate element proposed by Batoz and Katili [Batoz and Katili (1992)]
DKMT	Discrete Mindlin triangular plate element proposed by Katili [Katili (1993)]
DKT	The discrete Kirchhoff triangular plate element [Batoz, Bathe, and Ho (1980)]
RDKTM	Refined triangular plate element [Chen and Cheung (2001)]

4.1 Bending patch test

The patch test is a well-known benchmark to validate plate and shell elements. The geometry and mesh for the bending patch test are depicted in Figure 2, as well as nodal coordinates. The Young's modulus of the plate is 2.1×10^7 and Poisson's ratio $v = 0.3$ are used for the isotropic elastic material. Analytic field for thin plate bending is given by

$$w(x,y) = 0.001x^2 - 0.0003y^2 \tag{60}$$

The rotation can be calculated under the Kirchhoff assumptions as follows

$$\theta_x = \frac{\partial w}{\partial y} = -0.0006y \qquad \theta_y = -\frac{\partial w}{\partial x} = -0.002x \tag{61}$$

The exact transverse displacements and rotations are prescribed as essential boundary conditions in node 1-4. If the calculated displacements at the inner nodes 5-8 match the analytical displacements, the element pass the bending patch test. The calculated results under different thickness/width ratio given in Table 2 show that the present elements can pass the bending patch test.

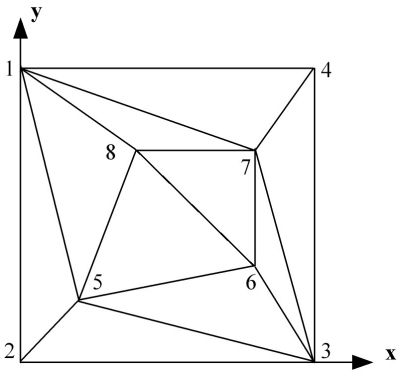

Node	X	Y
1	0.0	10.0
2	0.0	0.0
3	10.0	0.0
4	10.0	10.0
5	2.0	2.0
6	8.0	3.0
7	8.0	7.0
8	4.0	7.0

Figure 2: Mesh and nodal coordinates of the patch test.

Table 2: Thin plate patch test results under different thickness/width ratio. "P" represents pass.

Thickness/width ratio	0.4	0.2	0.1	0.01	0.001	0.0001
Thickness	4	2	1	0.1	0.01	0.001
QCS31	P	P	P	P	P	P
QCS32	P	P	P	P	P	P

4.2 Razzaque's skew plate

Figure 3(a) shows the geometry and material parameters for the Razzaque's skew plate subjected to a uniform load [Razzaque (1973)]. The problem serves to test the mesh distortion sensitivity of the element. The analytic solution and compared results of deflections at point C are shown in Table 3 and Figure 3(b). The results show that the present elements are competitive when compared with other elements.

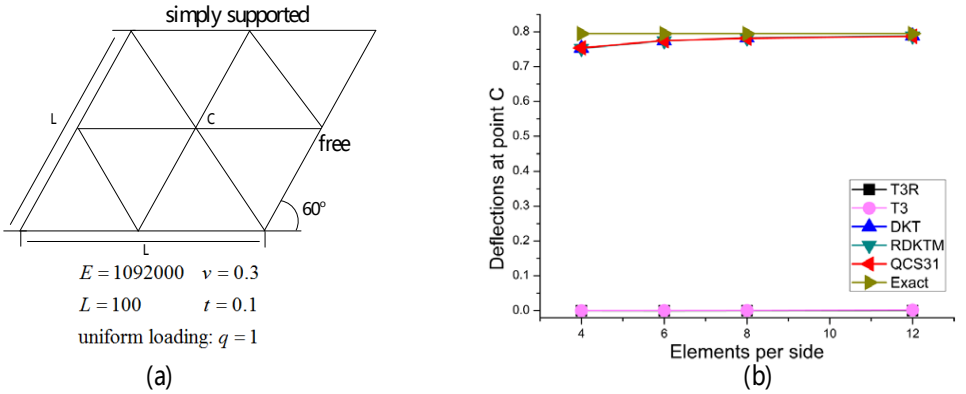

Figure 3: The Razzaque's skew plate

Table 3: Deflections at point C for the Razzaque's skew plate

	4×4	6×6	8×8	12×12
T3-R	0.0002	0.0005	0.0009	0.0020
T3	0.0001	0.0001	0.0002	0.0005
DKT	0.7527	0.7742	0.7822	0.7881
RDKTM	0.7527	0.7742	0.7822	0.7881
QCS31	0.7539	0.7745	0.7816	0.7868
Exact	0.7945			

4.3 Clamped square plate

Clamped square plate subjected to a uniformly distributed load is modeled to evaluate the ability of elimination of shear locking. Clamped boundary is applied on all four boundaries. The plate is divided into irregular meshes of 160 elements with various thickness/span ratios, as shown in Figure 4. The material and geometrical parameters used are Young's modulus $E = 1092$, Poisson's ratio $v = 0.3$, length of the plate $L = 10$, and the range of thickness/span ratios $t/L = 0.6 - 10^{-30}$. The results in Table 4 indicate that the present elements have very good properties of being free from shear locking.

4.4 Circular plate

A simply supported or clamped circular plate subjected to uniform loading is analyzed to demonstrate more features of the present elements. One quarter of the circular plate is modeled with three different elements meshes of 6, 24 and 96, as shown in Figure 5. The radius of the plate is $R = 5$ and different cases of the thick-

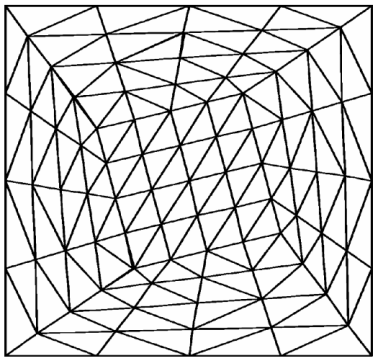

Figure 4: Clamped square plate discretized into irregular mesh (160 elements)

Table 4: Central deflection of the uniformly loaded whole clamped plate

t/L	0.6	0.4	0.25	0.2	0.05	10^{-2}	10^{-5}	10^{-7}	10^{-10}	10^{-15}	10^{-30}
T3-R	872.3	456.7	251.6	202.7	95.4	22.4	0.000	0.000	0.000	0.000	0.000
T3	871.7	455.4	248.5	198.1	64.8	5.1	0.000	0.000	0.000	0.000	0.000
DKT	130.6	130.6	130.6	130.6	130.6	130.6	130.6	130.6	130.6	130.6	130.6
RDKTM	886.4	471.5	267.8	220.2	136.9	130.9	130.6	130.6	130.6	130.6	130.6
QCS31	887.5	471.4	267.4	219.7	135.9	129.6	129.4	129.4	129.4	129.4	129.4
Exact							126.5	126.5	126.5	126.5	126.5

ness are investigated here. Poisson ratio $v = 0.3$ and Young's modulus $E = 10.92$. The compared results are listed in Table 5-8. Figure 6 shows the central deflections and moments of the clamped circular plate of thickness $t = 0.1$. The compared results show the present elements are competitive when compared with other elements.

4.5 Pinched cylinder

The pinched cylinder with diaphragm boundary conditions are subjected to a pair of opposite forces applied in the mid-span is an example commonly applied for the analysis of shell finite element formulations. This test is severe for both inextensional bending and complex membrane states. Due to the symmetry only one octant of the cylinder is modeled. The exact deflection at the location of the point C is 1.8248×10^{-5} [MacNeal and Harder (1985)]. The results of the present formulations and those of the references are shown in Figure 7 and Table 9. It can be seen that the present elements are very effective in this example.

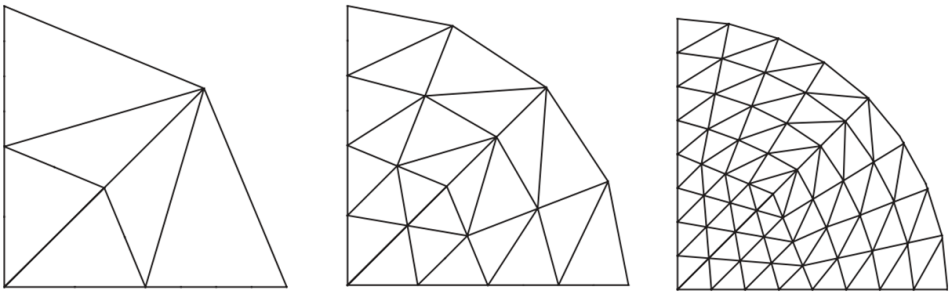

Figure 5: Different meshes of symmetrical quadrants of a circular plate

Table 5: Central deflection for a simply supported circular plate with a uniform load

	R/t=2			R/t=5			R/t=50		
	6	24	96	6	24	96	6	24	96
T3-R	2.534	3.073	3.219	27.487	36.778	40.251	2488.0	6500.6	15881.1
T3	2.298	2.984	3.195	15.804	30.195	38.032	282.7	1221.4	4507.0
DKT	2.421	2.520	2.524	37.833	39.378	39.714	37832.7	39378.2	39714.1
RDKTM	3.091	3.224	3.254	39.463	41.089	41.473	37848.5	39394.3	39730.2
QCS31	3.086	3.224	3.254	39.387	41.042	41.467	37771.3	39326.9	39716.2
Exact		3.262			41.599			39831	

Table 6: Central moment for a simply supported circular plate with a uniform load

	R/t=2			R/t=5			R/t=50		
	6	24	96	6	24	96	6	24	96
T3-R	3.798	4.760	5.073	3.275	4.363	5.026	0.351	0.693	2.851
T3	3.376	4.616	5.040	1.896	3.663	4.820	0.036	0.151	0.748
DKT	5.259	5.203	5.205	5.259	5.203	5.182	5.259	5.203	5.182
RDKTM	5.393	5.270	5.204	5.306	5.239	5.201	5.259	5.204	5.183
QCS31	5.431	5.312	5.210	5.332	5.275	5.220	5.279	5.221	5.183
Exact		5.16			5.16			5.16	

4.6 Hemispherical shell

A hemispherical shell with a top hole of 18° proposed by MacNeal and Harder[MacNeal and Harder (1985)] is shown in Figure 8(a). The problem is very useful to access the finite element ability to represent inextensional bending deformation modes

Table 7: Central deflection for a clamped circular plate with a uniform load

	R/t=2.5			R/t=5			R/t=50		
	6	24	96	6	24	96	6	24	96
T3-R	1.573	1.977	2.082	6.761	10.049	11.099	342.69	1370.8	3140.96
T3	1.445	1.911	2.060	4.575	8.401	10.467	70.81	274.38	925.54
DKT	1.286	1.246	1.229	10.291	9.966	9.835	10290.7	9966.1	9835.5
DKMT[Katili (1993)]	2.119	2.126	2.119	11.921	11.703	11.594	10306.0	9995.6	9847.5
DST-BK[Batoz and Katili (1992)]	2.043	2.112	2.114	11.342	11.548	11.554	9843.0	9855.1	9802.5
DST-BL[Batoz and Lardeur (1989)]	2.136	2.153	2.149	11.951	11.806	11.731	10306.0	9995.8	9848.3
RDKTM	2.119	2.124	2.119	11.921	11.687	11.598	10306.5	9982.4	9851.7
QCS31	2.077	2.123	2.118	11.591	11.656	11.581	9972.5	9940.2	9827.3
Exact		2.114			11.551			9783.5	

Table 8: Central moment for a clamped circular plate with a uniform load

	R/t=2.5			R/t=5			R/t=50		
	6	24	96	6	24	96	6	24	96
T3-R	1.338	1.846	1.986	1.186	1.735	1.956	0.080	0.307	0.838
T3	1.093	1.745	1.961	0.658	1.429	1.858	0.012	0.059	0.245
DKT	2.397	2.147	2.074	2.397	2.147	2.074	2.397	2.147	2.074
DKMT[Katili (1993)]	2.55	2.24	2.10	2.47	2.22	2.09	2.40	2.17	2.07
DST-BK[Batoz and Katili (1992)]	2.32	2.15	2.07	2.31	2.16	2.07	2.56	2.25	2.09
DST-BL[Batoz and Lardeur (1989)]	2.47	2.21	2.13	2.43	2.19	2.10	2.40	2.17	2.07
RDKTM	2.506	2.209	2.097	2.451	2.185	2.097	2.398	2.148	2.076
QCS31	2.514	2.250	2.101	2.440	2.219	2.098	2.386	2.165	2.075
Exact		2.03			2.03			2.03	

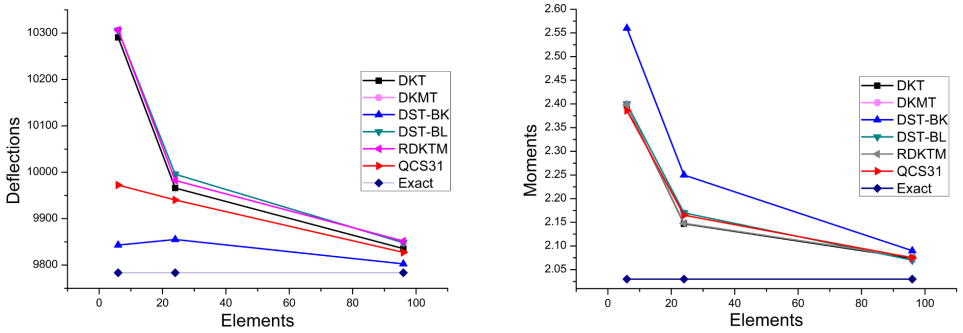

Figure 6: Central deflections and moments of a circular plate(clamped, uniform load and $R/t = 50$)

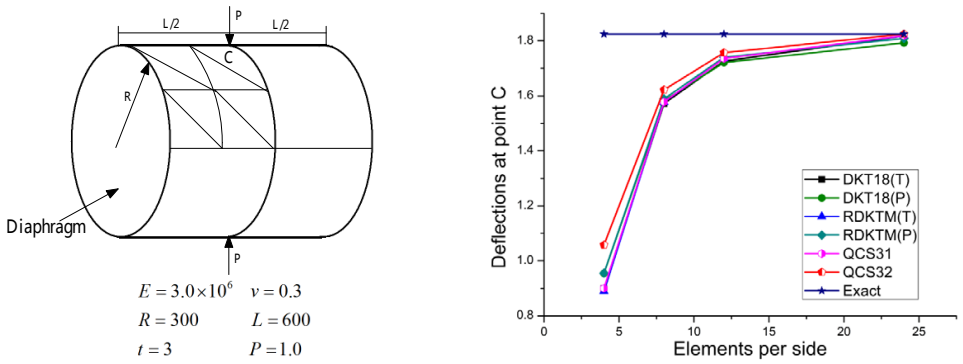

Figure 7: Pinched cylinder

Table 9: Deflections (10^{-5}) at point C for the pinched cylinder

	4×4	8×8	12×12	24×24
DKT18(T)	0.898	1.572	1.726	1.818
DKT18(P)	0.954	1.582	1.721	1.793
RDKTM(T)	0.889	1.577	1.736	1.818
RDKTM(P)	0.955	1.589	1.740	1.809
QCS31	0.900	1.578	1.736	1.819
QCS32	1.058	1.622	1.757	1.825
Exact	1.8248			

and rigid body rotation about the normal to the shell surface. Taking advantage of symmetry, only a quadrant of the shell is modeled. The analytic value for the displacement at point A is 0.094. Excellent results obtained when compare with the results from the references, which list in Table 10 and Figure 8(b). It can be seen that no membrane locking takes place in the problems for the present elements and the elements with constraints of the true drilling rotation freedom produce the best results.

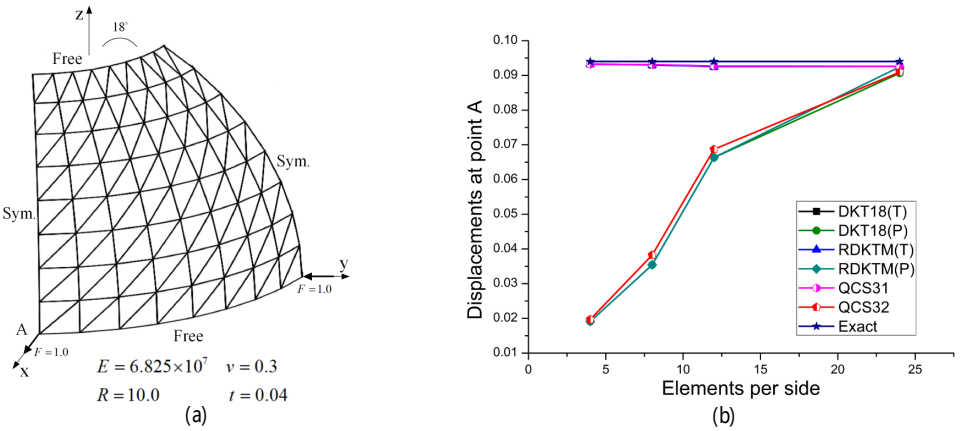

Figure 8: Hemispherical shell with 18° hole

Table 10: Displacements at point A for hemispherical shell with 18° hole

	4×4	8×8	12×12	24×24
DKT18(T)	0.09328	0.09300	0.09257	0.09260
DKT18(P)	0.01910	0.03541	0.06635	0.09064
RDKTM(T)	0.09328	0.09301	0.09258	0.09260
RDKTM(P)	0.01911	0.03542	0.06636	0.09247
QCS31	0.09319	0.09313	0.09270	0.09261
QCS32	0.01969	0.03825	0.06871	0.09094
Exact	0.094			

5 Conclusions

The QC technique has achieved great success in linear and nonlinear field of finite element analysis [Lomboy, Suthasupradit, Kim, and Oñate (2009)]. However, to

the best of our knowledge, few Reissner-Mindlin triangular QC elements have been developed. A Reissner-Mindlin quadrilateral shell element has been proposed by using Timoshenko's beam function [Wang, Hu, and Xia (2012)]. In this paper, we use Timoshenko's beam function to derive 3-node triangular Reissner-Mindlin flat shell elements within the framework of QC technique. From the preceding discussions and numerical examples, the following conclusions can be drawn:

(1) A series of new interpolation functions are deduced for the QC technique. The exact solution of Timoshenko's beam function is used successfully to derive the element, and the interpolated inner field function is obtained. The re-constitution technique for the shear strain terms is adopted for shear part. Both elements can be used for the analysis of both moderately thick and thin plates/shells, and the convergence for the very thin case can be ensured theoretically. The interpolation functions can also be used to construct geometric and material non-linearity elements.

(2) The advantages of QC technique are preserved: explicit stiffness matrix, convenient post-processing, free from membrane locking and shear locking. The numerical results show that the present elements provides good results to most problems when compared with referenced 3-node plates and shells elements.

Acknowledgement: This work was funded by the Key Project of the National Natural Science Foundation of China (No. 10932003, 11272075), "973"National Basic Research Project of China (No. 2010CB832700) and "04" Great Project of Ministry of Industrialization and Information of China (No. 2011ZX04001-021). These supports are gratefully acknowledged. Many thanks are due to the referees for their valuable comments.

References

Allman, D. J. (1984): A compatible triangular element including vertex rotations for plane elasticity analysis. *Computers & Structures*, vol. 19, no. 1-2, pp. 1–8.

Allman, D. J. (1988): Evaluation of the constant strain triangle with drilling rotations. *International Journal for Numerical Methods in Engineering*, vol. 26, no. 12, pp. 2645–2655.

Allman, D. J. (1991): Analysis of general shells by flat facet finite element approximation. *Aeronautical Journal*, vol. 95, pp. 194–203.

Allman, D. J. (1994): A basic flat facet finite element for the analysis of general shells. *International Journal for Numerical Methods in Engineering*, vol. 37, no. 1, pp. 19–35.

Alvin, K.; Fuente, H. M.; Haugen, B.; Felippa, C. A. (1992): Membrane triangles with corner drilling freedoms - part I. The EFF element. *Finite Elements in Analysis and Design*, vol. 12, no. 3-4, pp. 163–187.

Bathe, K. J.; Dvorkin, E. N. (1986): A formulation of general shell elements–the use of mixed interpolation of tensorial components. *International Journal for Numerical Methods in Engineering*, vol. 22, no. 3, pp. 697–722.

Bathe, K. J.; Ho, L. W. (1981): A simple and effective element for analysis of general shell structures. *Computers & Structures*, vol. 13, no. 5-6, pp. 673–681.

Batoz, J. L.; Bathe, K. J.; Ho, L. W. (1980): A study of three-node triangular plate bending elements. *International Journal for Numerical Methods in Engineering*, vol. 15, no. 12, pp. 1771–1812.

Batoz, J. L.; Katili, I. (1992): On a simple triangular Reissner/Mindlin plate element based on incompatible modes and discrete constraints. *International Journal for Numerical Methods in Engineering*, vol. 35, no. 8, pp. 1603–1632.

Batoz, J. L.; Lardeur, P. (1989): A discrete shear triangular nine D.O.F. element for the analysis of thick to very thin plates. *International Journal for Numerical Methods in Engineering*, vol. 28, no. 3, pp. 533–560.

Batoz, J. L.; Zheng, C. L.; Hammadi, F. (2001): Formulation and evaluation of new triangular, quadrilateral, pentagonal and hexagonal discrete Kirchhoff plate/shell elements. *International Journal for Numerical Methods in Engineering*, vol. 52, no. 5-6, pp. 615–630.

Bazeley, G. P.; Cheung, Y. K.; Irons, B. M.; Zienkiewicz, O. C. (1966): Triangular elements in plate bending, conforming and non-conforming solutions. *Proceedings of the First Conference on Matrix Methods in Structural Mechanics*, pp. 547–576.

Bergan, P. G.; Felippa, C. A. (1985): A triangular membrane element with rotational degrees of freedom. *Computer Methods in Applied Mechanics and Engineering*, vol. 50, no. 1, pp. 25 – 69.

Brezzi, F.; Marini, L. D. (2003): A nonconforming element for the Reissner-Mindlin plate. *Computers & Structures*, vol. 81, no. 8-11, pp. 515 – 522.

Chen, W. J. (2004): Refined 15-DOF triangular discrete degenerated shell element with high performances. *International Journal for Numerical Methods in Engineering*, vol. 60, no. 11, pp. 1817–1846.

Chen, W. J.; Cheung, Y. K. (1997): Refined quadrilateral discrete Kirchhoff thin plate bending element. *International Journal for Numerical Methods in Engineering*, vol. 40, no. 21, pp. 3937–3953.

Chen, W. J.; Cheung, Y. K. (2000): Refined quadrilateral element based on Mindlin/Reissner plate theory. *International Journal for Numerical Methods in Engineering*, vol. 47, no. 1-3, pp. 605–627.

Chen, W. J.; Cheung, Y. K. (2001): Refined 9-dof triangular Mindlin plate elements. *International Journal for Numerical Methods in Engineering*, vol. 51, no. 11, pp. 1259–1281.

Chen, W. J.; Cheung, Y. K. (2005): Refined discrete quadrilateral degenerated shell element by using Timoshenko's beam function. *International Journal for Numerical Methods in Engineering*, vol. 63, no. 8, pp. 1203–1227.

Cheung, Y. K.; Chen, W. J. (1995): Refined nine-parameter triangular thin plate bending element by using refined direct stiffness method. *International Journal for Numerical Methods in Engineering*, vol. 38, no. 2, pp. 283–298.

Cook, R. D. (1986): On the allman triangle and a related quadrilateral element. *Computers & Structures*, vol. 22, no. 6, pp. 1065 – 1067.

Cook, R. D. (1987): A plane hybrid element with rotational d.o.f. and adjustable stiffness. *International Journal for Numerical Methods in Engineering*, vol. 24, no. 8, pp. 1499–1508.

Dhatt, G.; Marcotte, L.; Matte, Y. (1986): A new triangular discrete Kirchhoff plate/shell element. *International Journal for Numerical Methods in Engineering*, vol. 23, no. 3, pp. 453–470.

Felippa, C. A. (2003): A study of optimal membrane triangles with drilling freedoms. *Computer Methods in Applied Mechanics and Engineering*, vol. 192, no. 16-18, pp. 2125–2168.

Felippa, C. A.; Alexander, S. (1992): Membrane triangles with corner drilling freedoms - part III. Implementation and performance evaluation. *Finite Elements in Analysis and Design*, vol. 12, no. 3-4, pp. 203 – 239.

Felippa, C. A.; Militello, C. (1992): Membrane triangles with corner drilling freedoms - part II. the ANDES element. *Finite Elements in Analysis and Design*, vol. 12, no. 3-4, pp. 189–201.

Ge, Z. J.; Chen, W. J. (2003): Refined triangular discrete Mindlin flat shell elements. *Computational Mechanics*, pp. 52–60.

Hu, P.; Xia, Y.; Tang, L. M. (2011): A four-node Reissner-Mindlin shell with assumed displacement quasi-conforming method. *CMES: Computer Modeling in Engineering and Sciences*, vol. 73, no. 2, pp. 103–136.

Hughes, T. J. R.; Cohen, M.; Haroun, M. (1978): Reduced and selective integration techniques in the finite element analysis of plates. *Nuclear Engineering and Design*, vol. 46, no. 1, pp. 203–222.

Katili, I. (1993): A new discrete Kirchhoff-Mindlin element based on Mindlin-Reissner plate theory and assumed shear strain fields - part I: An extended DKT element for thick-plate bending analysis. *International Journal for Numerical Methods in Engineering*, vol. 36, no. 11, pp. 1859–1883.

Kim, K. D.; Lomboy, G. R.; Voyiadjis, G. Z. (2003): A 4-node assumed strain quasi-conforming shell element with 6 degrees of freedom. *International Journal for Numerical Methods in Engineering*, vol. 58, no. 14, pp. 2177–2200.

Kim, S. H.; Choi, C. K. (1992): Improvement of quadratic finite element for Mindlin plate bending. *International Journal for Numerical Methods in Engineering*, vol. 34, no. 1, pp. 197–208.

Lee, S. W.; Plan, T. H. H. (1978): Improvement of plate and shell finite elements by mixed formulations. *AIAA Journal*, vol. 16, pp. 29–34.

Liu, Y. X.; Shi, G. Y.; Tang, L. M. (1983): Discussion on the superfluous zero energy modes of finite elements (in Chinese). *Journal of Dalian Institute of Technology*, vol. 22, no. 3, pp. 62–67.

Lomboy, G. R.; Suthasupradit, S.; Kim, K. D.; Oñate, E. (2009): Nonlinear formulations of a four-node quasi-conforming shell element. *Archives of Computational Methods in Engineering*, vol. 16, pp. 189–250.

Lv, H. X.; Xu, S. N. (1989): An effective quadrilateral plate bending element. *International Journal for Numerical Methods in Engineering*, vol. 28, no. 5, pp. 1145–1160.

MacNeal, R. H. (1982): Derivation of element stiffness matrices by assumed strain distributions. *Nuclear Engineering and Design*, vol. 70, no. 1, pp. 3 – 12.

MacNeal, R. H.; Harder, R. L. (1985): A proposed standard set of problems to test finite element accuracy. *Finite Elements in Analysis and Design*, vol. 1, no. 1, pp. 3 – 20.

Meek, J. L.; Tan, H. S. (1985): A discrete Kirchoff plate bending element with loof nodes. *Computers & Structures*, vol. 21, no. 6, pp. 1197–1212.

Pugh, E. D., H. E.; Zienkiewicz, O. C. (1978): A study of triangular plate bending element with reduced integration. *International Journal for Numerical Methods in Engineering*, vol. 12, no. 7, pp. 1059–1078.

Razzaque, A. (1973): Program for triangular bending elements with derivative smoothing. *International Journal for Numerical Methods in Engineering*, vol. 6, no. 3, pp. 333–343.

Shi, G. Y.; Voyiadjis, G. Z. (1991): Efficient and accurate four-node quadrilateral C^0 plate bending element based on assumed strain fields. *International Journal for Numerical Methods in Engineering*, vol. 32, no. 5, pp. 1041–1055.

Simo, J. C.; Rifai, M. S. (1990): A class of mixed assumed strain methods and the method of incompatible modes. *International Journal for Numerical Methods in Engineering*, vol. 29, no. 8, pp. 1595–1638.

Spilker, R. L.; Munir, N. I. (1980): A hybrid-stress quadratic serendipity displacement Mindlin plate bending element. *Computers & Structures*, vol. 12, no. 1, pp. 11 – 21.

Tang, L. M.; Chen, W. J.; Liu, Y. X. (1980): Quasi-conforming elements for finite element analysis (in Chinese). *Journal of Dalian Institute of Technology*, vol. 2, pp. 17–35.

Tang, L. M.; Chen, W. J.; Liu, Y. X. (1981): The quasi-conforming element method for thin plate bending analysis (in Chinese). *Journal of Building Structures*, vol. 2, pp. 10–22.

Tang, L. M.; Chen, W. J.; Liu, Y. X. (1983): String net function application and quasi-conforming technique. *Hybrid and Mixed Finite Element Methods, Alturi SN et al. (ed.), Wiley: New York.*

Wang, C. S.; Hu, P.; Xia, Y. (2012): A 4-node quasi-conforming Reissner Mindlin shell element by using Timoshenko's beam function. *Finite Elements in Analysis and Design*, vol. 61, pp. 12 – 22.

Zhang, Y.; Zhou, H. M.; Li, J. H.; Feng, W.; Li, D. Q. (2011): A 3-node flat triangular shell element with corner drilling freedoms and transverse shear correction. *International Journal for Numerical Methods in Engineering*, vol. 86, no. 12, pp. 1413–1434.

Zienkiewicz, O. C. (1977): The finite element method(3rd edition). *McGraw-Hill, New Jersey*.

Zienkiewicz, O. C.; Taylor, R. L.; Too, J. M. (1971): Reduced integration technique in general analysis of plates and shells. *International Journal for Numerical Methods in Engineering*, vol. 3, no. 2, pp. 275–290.